







Synechococcus sp. PCC7002 Uses Peroxiredoxin to Cope with Reactive Sulfur Species Stress

Daixi Liu,^{a,c} Jinyu Chen,^{a,c} Yafei Wang,^{a,c} Yue Meng,^{a,c} Yuanning Li,^{a,c} Ranran Huang,^{a,c}  Yongzhen Xia,^b  Huaiwei Liu,^b Nianzhi Jiao,^{a,c,d}  Luying Xun,^{b,e}  Jihua Liu^{a,c,d}

^aInstitute of Marine Science and Technology, Shandong University, Qingdao, People's Republic of China

^bState Key Laboratory of Microbial Technology, Shandong University, Qingdao, People's Republic of China

^cJoint Lab for Ocean Research and Education at Dalhousie University, Shandong University and Xiamen University

^dInstitute of Marine Microbes and Ecospheres, Xiamen University, Xiamen, China

^eSchool of Molecular Biosciences, Washington State University, Pullman, Washington, USA

ABSTRACT Cyanobacteria are a widely distributed group of microorganisms in the ocean, and they often need to cope with the stress of reactive sulfur species, such as sulfide and sulfane sulfur. Sulfane sulfur refers to the various forms of zero-valent sulfur, including persulfide, polysulfide, and element sulfur (S_8). Although sulfane sulfur participates in signaling transduction and resistance to reactive oxygen species in cyanobacteria, it is toxic at high concentrations and induces sulfur stress, which has similar effects to oxidative stress. In this study, we report that *Synechococcus* sp. PCC7002 uses peroxiredoxin to cope with the stress of cellular sulfane sulfur. *Synechococcus* sp. PCC7002 contains six peroxiredoxins, and all were induced by S_8 . Peroxiredoxin I (PrxI) reduced S_8 to H_2S by forming a disulfide bond between residues Cys⁵³ and Cys¹⁵³ of the enzyme. A partial deletion strain of *Synechococcus* sp. PCC7002 with decreased copy numbers of the *prxI* gene was more sensitive to S_8 than was the wild type. Thus, peroxiredoxin is involved in maintaining the homeostasis of cellular sulfane sulfur in cyanobacteria. Given that peroxiredoxin evolved before the occurrence of O_2 on Earth, its original function could have been to cope with reactive sulfur species stress, and that function has been preserved.

IMPORTANCE Cyanobacteria are the earliest microorganisms that perform oxygenic photosynthesis, which has played a key role in the evolution of life on Earth, and they are the most important primary producers in the modern oceans. The cyanobacterium *Synechococcus* sp. PCC7002 uses peroxiredoxin to reduce high levels of sulfane sulfur. That function is possibly the original role of peroxiredoxin, as the enzyme evolved before the appearance of O_2 on Earth. The preservation of the reduction of sulfane sulfur by peroxiredoxin5-type peroxiredoxins may offer cyanobacteria an advantage in the complex environment of the modern oceans.

KEYWORDS peroxiredoxin, reactive sulfur species, cyanobacteria, sulfane sulfur reduction

Cyanobacteria are one of the most important microbial groups; they provided the first source of O_2 on Earth via oxygenic photosynthesis (1, 2). However, some environments that cyanobacteria inhabit periodically experience decreased oxygen levels. Cyanobacterial mats are one environment with periodically anoxic conditions, in which cyanobacteria perform oxygenic photosynthesis in the daytime and turn to respiration in the dark. The insufficient diffusion of O_2 into the mat makes the mat turn anoxic. As a result, heterotrophic bacteria in the mat perform sulfate respiration and produce hydrogen sulfide (H_2S). Cyanobacteria can use H_2S as an electron donor to perform anoxygenic photosynthesis when oxygenic photosynthesis is inhibited by high concentrations of H_2S . Tons of sulfane

Editor Yong-Sun Bahn, Yonsei University

Copyright © 2022 Liu et al. This is an open-access article distributed under the terms of the [Creative Commons Attribution 4.0 International license](https://creativecommons.org/licenses/by/4.0/).

Address correspondence to Jihua Liu, liujihua1982@sdu.edu.cn.

The authors declare no conflict of interest.

Received 24 May 2022

Accepted 7 July 2022

Published 21 July 2022

sulfur may be produced by the oxidation of H_2S via sulfide:quinone oxidoreductase (SQR) in the mats (3, 4). Sulfane sulfur refers to the various forms of zero-valent sulfur, including persulfide, polysulfide, and elemental sulfur (S_8). Cyanobacteria inhabiting oxygen minimum zones (OMZs), where H_2S is sporadically accumulated, also face low- O_2 and sulfidic conditions. Moreover, cyanobacteria encounter sulfur in the photic zones above OMZs, which are even visible as “clouds” on satellite images. Sulfane sulfur is also likely to be abundant in the benthic realm (5, 6). H_2S and sulfane sulfur are two of the most important reactive sulfur species (RSS) that tend to be present in sulfidic conditions. RSS are a diverse class of sulfur-containing compounds and functional groups with important roles in chemical biology and bioinorganic chemistry (7–10). Therefore, cyanobacteria need to cope with the RSS stress caused by high concentrations of H_2S and the accumulation of sulfane sulfur in the environments discussed above (11, 12).

Sulfane sulfur, including persulfide forms (RSSH and HSSH), polysulfide forms (RSS_nH , RSS_nR , and H_2S_n , $n \geq 2$), and elemental sulfur (S_8), is commonly present in the cytoplasm of living organisms and plays important roles in maintaining intracellular redox homeostasis and metabolic regulation (7, 13–15). However, a high concentration of sulfane sulfur is toxic to cells and causes protein persulfidation and disulfide bond formation (16, 17). Inorganic polysulfides generated from organosulfur compounds inhibit several types of pathogenic and drug-resistant bacteria (18). Elemental sulfur is used as a potential antifungal agent (19). Consequently, cells have various enzymes and regulatory systems to protect against excessive levels of sulfane sulfur (20).

In some sulfidic environments, cyanobacteria can perform anoxygenic photosynthesis by using H_2S as an electron donor, and the key enzyme in this process is SQR (1, 21–23). Cyanobacteria SQR and peroxidase dioxygenase (PDO) can work together to detoxify H_2S (24). PDO is normally involved in the oxidation of the sulfane sulfur that is produced by SQR, but it functions at high levels of cellular sulfane sulfur. Other pathways that help to maintain the homeostasis of sulfane sulfur in cyanobacteria remain to be explored, considering the important role of sulfane sulfur in cellular signaling (25).

Microorganisms have evolved a series of mechanisms by which to maintain the homeostasis of intracellular sulfane sulfur. Besides PDO (26, 27), thioredoxins (Trx) and glutaredoxins (Grx) also reduce sulfane sulfur to H_2S (28–31). Furthermore, some cyanobacteria are capable of sulfur respiration, using elemental sulfur as an electron acceptor in dark and anoxic conditions (3, 32, 33). Moreover, catalase, which typically catalyzes the disproportionation of H_2O_2 to H_2O and O_2 (34, 35), also has the ability to oxidize inorganic persulfide (H_2S_2), which is structurally similar to H_2O_2 (36). Because peroxiredoxin (Prx) also uses H_2O_2 as a substrate (37–39), an immediate question is whether Prx can metabolize sulfane sulfur.

Prxs are ubiquitous in plants, animals, and bacteria (38, 40–43). Their active Cys residue is oxidized to sulfonic acid by H_2O_2 and organic peroxides. Depending on whether one or two Cys residues are involved in the process of recycling sulfonic acid back to the thiol form, they can be divided into three categories: typical 2-Cys Prxs, atypical 2-Cys Prxs, and 1-Cys Prxs (40, 44, 45). However, this classification was not unequivocally accepted. Kimberly et al. developed a method that used the Deacon Active Site Profiler tool to extract functional site (PXXXTXXC_p) profiles from structurally characterized Prxs and classify the Prxs into six distinct subclasses (46, 47): alkyl hydroperoxide reductase subunit C (AhpC-Prx), bacterioferritin comigratory protein (BCP-PrxQ), alkyl hydroperoxide reductase subunit E (AhpE), peroxiredoxin 5 (Prx5), peroxiredoxin 6 (Prx6), and thiol peroxidase (Tpx). Because inorganic polysulfide (H_2S_n) and H_2O_2 are structural analogs, we hypothesize that Prx can also metabolize H_2S_n . From the perspective of evolution, the origin of Prxs precedes the appearance of O_2 on Earth (48). Therefore, Prx might have been used to manage intracellular RSS before the appearance of O_2 and may offer cyanobacteria the advantage of being able to move in and out of hypoxic areas in the modern ocean (49–51).

Synechococcus sp. PCC7002 (PCC7002) contains six hypothetical Prxs: PrxI (ACA98797.1), PrxII (ACA98565.1), PrxIII (ACA99108.1), PrxIV (ACA98330.1), PrxV (ACA98124.1), and PrxVI

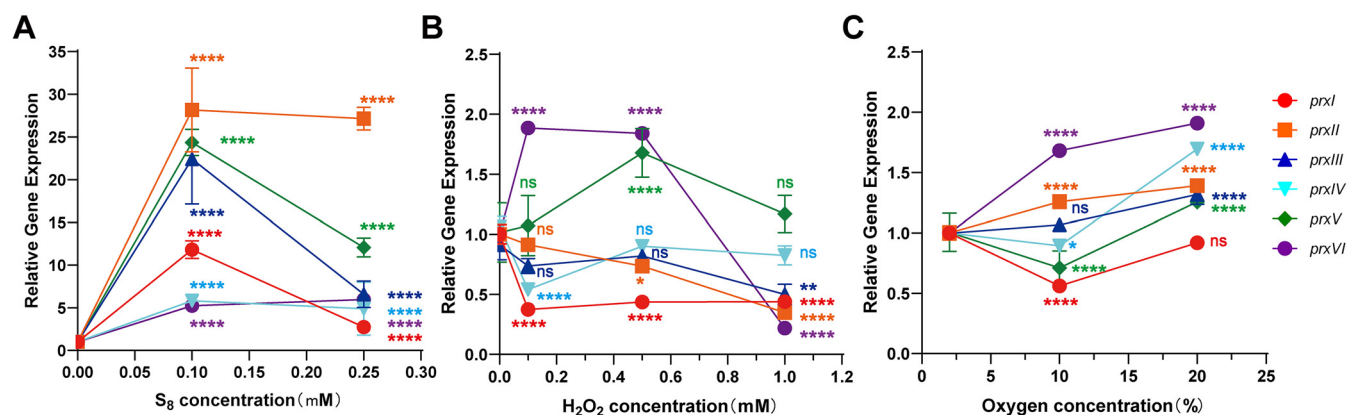


FIG 1 The effects of S_8 , H_2O_2 , and O_2 on the expression of *prxs* in PCC7002. The expression levels of *prxI*, *prxII*, *prxIII*, *prxIV*, *prxV*, and *prxVI* were measured using RT-qPCR after induction by S_8 (A) and H_2O_2 (B) for 3 h. (C) The expression of *prxs* in PCC7002 incubated under 2%, 10%, and 20% O_2 in the gas phase. To determine the expression levels of *prxs*, relative quantitative PCR was used. The relative gene expression represented the *prx* expression levels, standardized by the reference gene *rpnA*. All data are averages from three samples with standard deviations shown (error bars). The experiment was repeated at least three times. *, *P* value < 0.1; **, *P* value < 0.01; ***, *P* value < 0.001; ****, *P* value < 0.0001; ns, not significant (paired t-test).

(ACA99379.1). Among these, the role of PrxI in H_2O_2 metabolism has been confirmed (52). Here, we report that the Prxs in PCC7002 are all induced by S_8 . However, only PrxI was able to reduce S_8 to H_2S . The Cys⁵³ and Cys¹⁵³ residues of PrxI play critical roles in the reduction of sulfane sulfur to H_2S via the formation of a disulfide bond. PrxI, which belongs to the Prx5 subfamily, was distinct from the other Prxs of PCC7002 in a phylogenetic analysis. These results improve our understanding of the sulfane sulfur metabolic pathway of cyanobacteria, provide some explanation for the widespread distribution of cyanobacteria in the modern ocean, and provide a new perspective from which to explore the important role of cyanobacteria in the early evolution of life on Earth.

RESULTS

Sulfane sulfur upregulates the expression of *prxs* in PCC7002. Sulfane sulfur plays an important role in the regulation of the gene expression associated with photosynthesis in PCC7002, but it is toxic at high concentrations (24). S_8 at the concentrations of 500 μM and 1 mM were fatal to PCC7002 (Fig. S1). Then, 100 and 250 μM S_8 were used to induce PCC7002, and the expression of *prxs* were detected. All six *prxs* in PCC7002 were upregulated after induction by S_8 , as determined by a quantitative polymerase chain reaction (qPCR) analysis at all tested concentrations (Fig. 1A). At the concentration of 100 μM , the expression levels of *prxIV* and *prxVI* were upregulated by approximately 5-fold. The expression of *prxI* was increased notably (>10-fold). Furthermore, the expressions of *prxII*, *prxIII*, and *prxV* levels were also increased notably (from 20-fold to 30-fold). All *prxs* were also significantly upregulated at the concentration of 200 μM , although the amplitudes were not as high as those observed at 100 μM . Under reactive oxygen species (ROS) pressure, the expression of *prxs* changed slightly, by a maximum of about 2-fold after H_2O_2 induction (Fig. 1B) or incubation under 2%, 10%, or 20% O_2 (Fig. 1C).

PrxI metabolized S_8 and produced H_2S . To compare the functions of Prxs, H_2S production by recombinant Prxs fused to the C-terminus of MBP was detected (Fig. 2). Prxs with His-tags were found to be insoluble. First, 100 $\mu g/mL$ purified Prx-MBP fusion protein (Fig. S2A) were incubated with 200 μM elemental sulfur (S_8) and 100 μM dithiothreitol (DTT) for 5 min at 30°C in 50 mM HEPES buffer (pH 7.0). About 90 μM H_2S was released by Prx-MBP, while the H_2S production by PrxII through PrxVI was not significantly different from that of a control that contained only 200 μM S_8 and 100 μM DTT in HEPES buffer (Fig. 2A). Second, 200 μM S_8 were added to cell lysates of recombinant *E. coli* BL21 expressing Prx-MBP fusion (10 mg of protein mL^{-1}). An SDS-PAGE analysis showed a similar amount of the fused proteins in each sample (Fig. S2B). The lysate of recombinant *E. coli* BL21 expressing the PrxI fusion protein released about

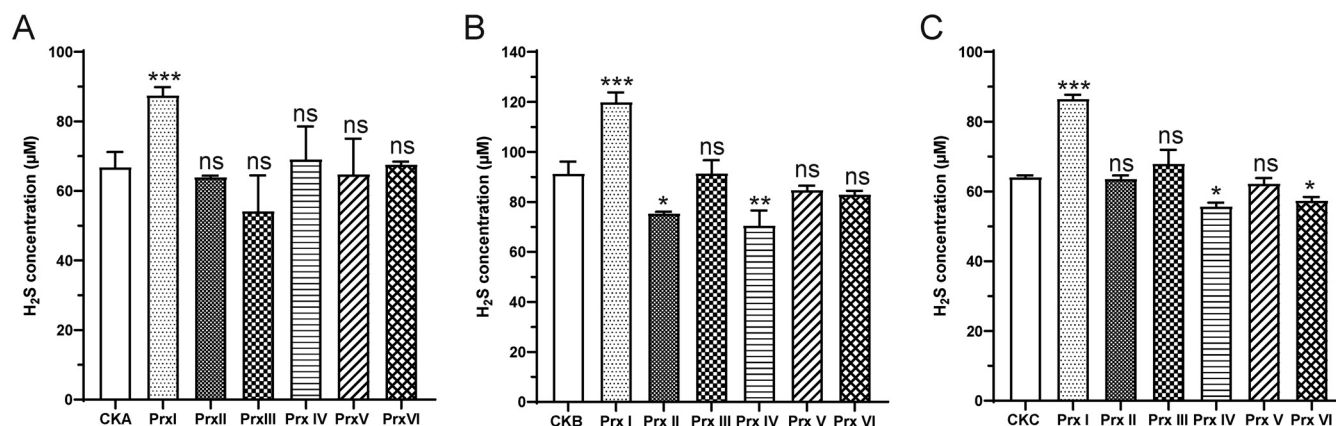


FIG 2 The metabolism of S₈ by Prxs. (A) The production of H₂S by purified PrxI-MBP, Prx II-MBP, Prx III-MBP, Prx IV-MBP, Prx V-MBP, and Prx VI-MBP. 100 µg/mL purified Prx-MBP was incubated with 200 µM elemental sulfur (S₈) and 100 µM DTT for 15 min at 30°C in 50 mM HEPES buffer (pH 7.0). CKA is represented the HEPES buffer with 200 µM elemental sulfur (S₈) and 100 µM DTT. (B) The production of H₂S by the lysates of the recombinant *E. coli* BL21 (DE3) (pMal-C2X) (CKB), *E. coli* BL21 (DE3) (pMal-*prxI*) (Prx I), *E. coli* BL21 (DE3) (pMal-*prxII*) (Prx II), *E. coli* BL21 (DE3) (pMal-*prxIII*) (Prx III), *E. coli* BL21 (DE3) (pMal-*prxIV*) (Prx IV), *E. coli* BL21 (DE3) (pMal-*prxV*) (Prx V), and *E. coli* BL21 (DE3) (pMal-*prxVI*) (Prx VI), with a total protein concentration of 10 mg/mL. 200 µM S₈ was used as the source of sulfane sulfur, and the treatment time was 5 min. (C) The production of H₂S by recombinant *E. coli* BL21 (DE3) (pMal-C2X) (CKC) and *E. coli* BL21 (DE3) (pMal-*prxI-VI*) cells. The recombinant *E. coli* BL21 strains were harvested and resuspended to an OD_{600 nm} of 10, and then 200 µM S₈ was added to initiate the reaction. The treatment time was 15 min. All data are averages from three samples with standard deviations shown (error bars). The experiment was repeated at least three times. *, *P* value < 0.1; **, *P* value < 0.01; ***, *P* value < 0.001; ****, *P* value < 0.0001; ns, not significant (paired *t*-test).

130 µM H₂S in 5 min of incubation. The control *E. coli* BL21 with empty vector pMal-C2X released only 90 µM H₂S. Compared to the control, no more H₂S was released by the lysates containing PrxII through PrxVI (Fig. 2B). Third, the ability of resting cells expressing Prx-MBP fusion protein to metabolize S₈ and produce H₂S was also measured, and only the resting cells with the PrxI-MBP fusion protein produced more H₂S than did the control cells with the empty vector (Fig. 2C). Thus, PrxI clearly reduced sulfane sulfur to H₂S.

A previously reported CstR-mKate reporter (53) was adapted to analyze the function of PCC7002 PrxI and its Cys residues. The reporter system included CstR and mKate, in which CstR inhibits the expression of *mkate*. Sulfane sulfur could relieve the inhibitory effect of CstR. Thus, the fluorescence intensity of mKate in the *E. coli* host cells could serve as an indicator of the levels of intracellular sulfane sulfur (Fig. 3A1), reaching a maximum when *E. coli* cells entered the early stationary phase (25). When *prxI* was cloned behind *mkate*, the mKate fluorescence was decreased because of the metabolism of sulfane sulfur by PrxI (Fig. 3A2). PrxI contains three cysteine residues (Cys⁵³, Cys⁷⁸ and Cys¹⁵³), and they were individually mutated to serine (Ser). The mKate fluorescence intensity in the modified reporter system with PrxI C78S was slightly higher than that in the system with wild-type PrxI. However, the mKate fluorescence intensities with PrxI C53S and PrxI C153S were significantly enhanced compared with those for the construct containing PrxI, and the control without PrxI had the highest mKate fluorescence (Fig. 3A2). Thus, the mutation of Cys⁵³ and Cys¹⁵³ destroyed the ability of PrxI to reduce sulfane sulfur.

Furthermore, the Cys residues of PrxI in pMal-C2X were also individually mutated to Ser. Purified PrxI-MBP C53S and PrxI-MBP C153S produced less H₂S than did wild-type PrxI-MBP and PrxI-MBP C78S, indicating the importance of Cys⁵³ and Cys¹⁵³ (Fig. 3B and Fig. S3A). Meanwhile, the lysate of *E. coli* BL21 cells expressing PrxI-MBP C53S or PrxI-MBP C153S also produced less H₂S from added S₈ than did cells expressing wild-type PrxI-MBP or PrxI-MBP C78S (Fig. 3C). The cell lysates of the *E. coli* BL21 expressing PrxI-MBP and its mutants were standardized by protein concentration and were confirmed to contain similar amounts of proteins by an SDS-PAGE analysis (Fig. S3B).

We tested whether the Cys⁵³ and Cys¹⁵³ of PrxI formed a disulfide bond. The MBP fusion proteins were purified and cleaved by Factor Xa to release PrxI, PrxI C53S, PrxI C78S, and PrxI C153S. The released Prx proteins were analyzed by non-reducing SDS-

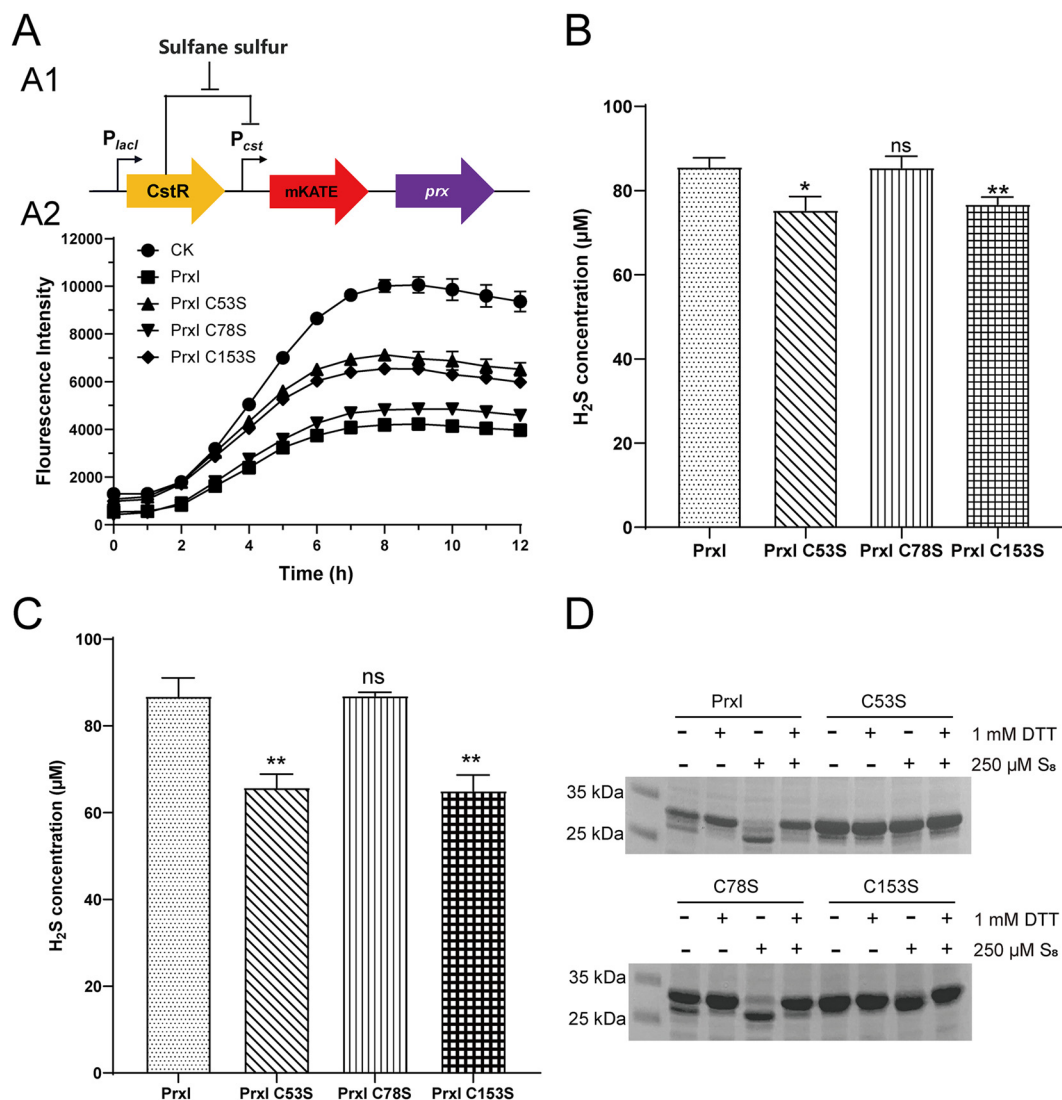


FIG 3 The metabolism of S₈ by PrxI and its mutants. (A) The function of PrxI detected by the CstR-reporter system. (A1) The schematic diagram of the CstR-reporter system. The CstR reporter system was built to access the activities of Prxs, in which H₂S₈ could relieve the repression of *mkate* by CstR. The mKate fluorescence was used to characterize the abilities of Prxs to metabolize sulfane sulfur. (A2) The fluorescence intensities of mKate in the CstR-reporter system coupled with PrxI and its cysteine mutants. (B) The production of H₂S by purified PrxI, PrxI C53S, PrxI C78S, and PrxI C153S. (C) The production of H₂S by lysates of recombinant *E. coli* BL21 (DE3) cells expressing *prxI* and its cysteine mutants. (D) Nonreducing SDS-PAGE of PrxI, PrxI C53S, PrxI C78S, and PrxI C153S after S₈ and DTT treatment. The proteins were cleaved from the MBP-fusion proteins by Factor Xa at room temperature for 24 h, and 6 μg of PrxI proteins were loaded. All data are averages from three samples with standard deviations shown (error bars). The experiment was repeated at least three times. *, *P* value < 0.1; **, *P* value < 0.01; ns, not significant (paired *t*-test).

PAGE. In the SDS-PAGE, untreated PrxI and PrxI C78S showed two bands, with the upper band being dominant. The upper band was converted to the lower band upon treatment with 250 μM S₈. PrxI C53S and PrxI C153S showed only the upper band, and S₈ treatment did not affect it (Fig. 3D). The upper band represented the PrxI protein without an intramolecular disulfide bond, while the lower band represented the protein with an intramolecular disulfide bond. All modifications were converted back to thiols by treatment with DTT. Hence, the Cys⁵³ and Cys¹⁵³ of PrxI are involved in reducing S₈ to H₂S, and they form an intramolecular disulfide bond.

PrxI enhanced the survival of PCC7002 after sulfane sulfur exposure. The deletion of *prxI* affected the survival of PCC7002 after sulfane sulfur exposure. We tried to construct a single deletion strain by homologous recombination. However, *prxI* could only be partially knocked out (to give strain PCC7002Δ*prxI*-p), as the kanamycin-

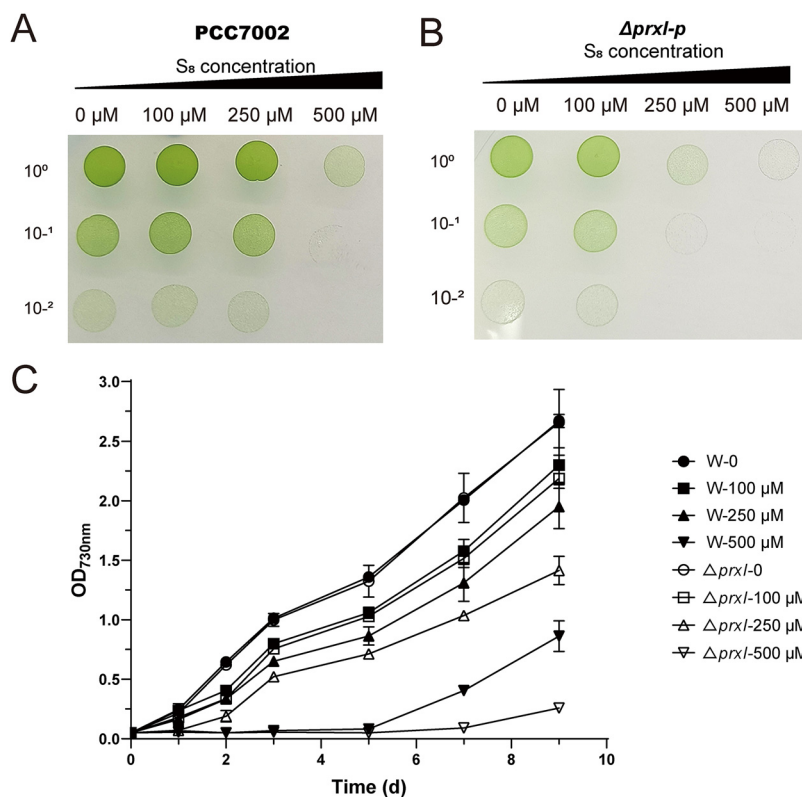
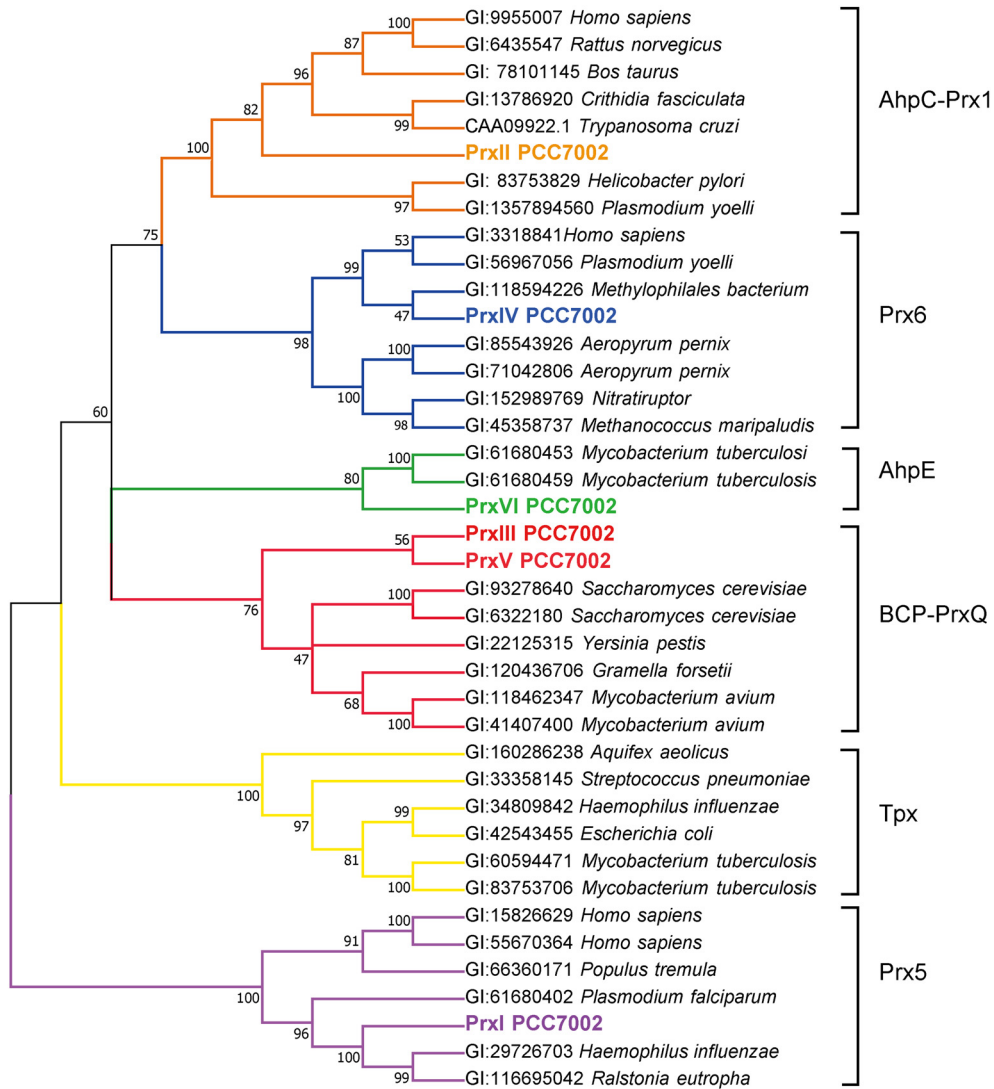


FIG 4 The tolerance of PCC7002 and PCC7002 $\Delta prxl$ -p to S_8 -treatment. The growth of the wild type PCC7002 (A) and its *prxl* partial deletion mutant, PCC7002 $\Delta prxl$ -p, (B) on the A⁺ agar plate after incubation with 100, 250, and 500 μM S_8 . The cells with an OD_{730nm} of 0.05 were treated with S_8 under 30°C and 50 μmol photons $m^{-2} s^{-1}$ illumination for 6 h. Then, the treated cells were diluted with A⁺ medium to 10⁰, 10⁻¹, and 10⁻², then placed on the A⁺ plate for a further cultivation of 7 days under 30°C and 50 μmol photons $m^{-2} s^{-1}$ illumination. (C) The growth curve of PCC7002 and PCC7002 $\Delta prxl$ -p in the presence of S_8 . PCC7002 showed a higher resistance to S_8 treatment than did PCC7002 $\Delta prxl$ -p. All data are averages from three samples with standard deviations shown (error bars). The experiment was repeated at least three times.

resistant mutant contained both the intact *prxl* gene and the kanamycin resistance gene when checked by PCR (Fig. S4). Cyanobacteria often have multiple chromosomes per cell (54), and many critical genes cannot be completely deleted from all chromosomes, as that would be fatal to the cell. Because *prxl* could not be completely deleted, PrxI is likely to play an essential physiological role in PCC7002. Even though not all copies of *prxl* were knocked out, the mutant showed a distinct response to S_8 exposure compared to that of the wild type. PCC7002 and PCC7002 $\Delta prxl$ -p cells were treated with various amounts of S_8 for 6 h and then placed on A⁺ agar. After culturing for 7 days, PCC7002 grew well at the S_8 concentration of 250 μM (Fig. 4A), while the growth of PCC7002 $\Delta prxl$ -p was largely inhibited at that concentration (Fig. 4B). At 500 μM S_8 , PCC7002 could grow in small colonies, while PCC7002 $\Delta prxl$ -p was completely inhibited. Furthermore, the growth curves of PCC7002 and PCC7002 $\Delta prxl$ -p were monitored in the presence of 0, 100, 250, and 500 μM S_8 (Fig. 4C). The growth curve of PCC7002 and PCC7002 $\Delta prxl$ -p was similar in the absence of S_8 . PCC7002 grew better than PCC7002 $\Delta prxl$ -p did in the presence of 100, 250, and 500 μM S_8 . The above results indicate that PrxI plays a critical role in the survival of PCC7002 after exposure to S_8 .

Phylogenetic analysis of Prxs in PCC7002. We conducted a phylogenetic analysis of the six Prxs in PCC7002 (Fig. 5A). Based on an analysis using the Deacon Active Site Profiler tool, Prxs are classified into six subfamilies (47). Here, representative sequences from each subfamily were selected to analyze the classification of the Prxs in PCC7002 (Table S3). The Prxs in PCC7002 belonged to five subfamilies: PrxI belonged to the Prx5 subfamily, PrxII belonged to the AhpC-Prx1 subfamily, PrxIII and PrxV belonged to the

A



B

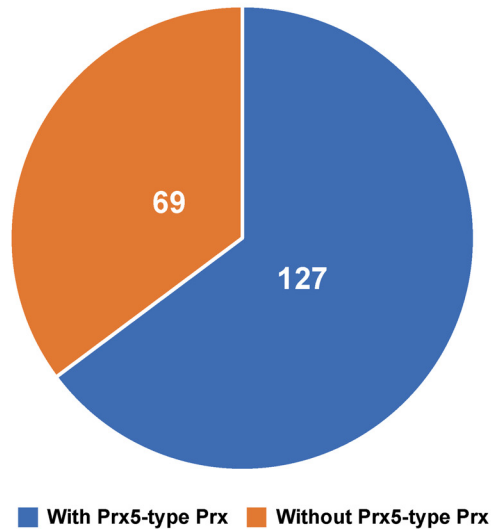


FIG 5 Phylogenetic analysis of Prxs in Cyanobacteria. (A) The genetic diversity of Prxs in PCC7002. The six Prxs in PCC7002 were divided into five subclasses: PrxI PCC7002 belonged to the Prx5 family, PrxII PCC7002 belonged to the

(Continued on next page)

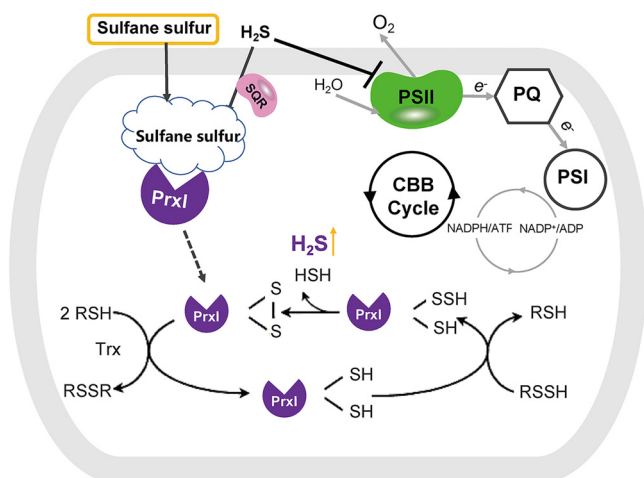


FIG 6 PeroxiredoxinI metabolized S₈ and produced H₂S. The expressions of *prxs* in PCC7002 are induced by S₈. Among these, PrxI reduces S₈ to H₂S by donating an electron, thereby generating a disulfide bond between Cys⁵³ and Cys¹⁵³. Thioredoxin (Trx) then reduces the disulfide bond. As a result, PrxI helps PCC7002 to cope with the reactive sulfur species stress in the living environments.

BCP-PrxQ subfamily, PrxVI belonged to the AhpE subfamily, and PrxIV belonged to the Prx6 subfamily. There is no Prx in PCC7002 belonging to the Tpx subfamily. Although the Prx5 subfamily was significantly different from the other subfamilies, as evidenced by it occupying a separate branch in the phylogenetic tree (Fig. 5A), the sequence around the active site of Prx5 subfamily members (PXXXTXXC_p, where C_p is the Cys⁵³ of PrxI) is highly conserved (Fig. S5A). Based on the above findings, we deduced that the sequence specificity of PrxI determined its activity.

Currently, 198 genomes of cyanobacteria have been sequenced, and we searched them for Prxs, using the queries in Table S3. There were 1,272 probable Prxs in these cyanobacteria, of which 194 belonged to the AhpC-Prx subfamily, 148 to the Prx6 subfamily, 189 to the AhpE subfamily, 612 to the BCP-PrxQ subfamily, and 129 to the Prx5 subfamily (Table S4). No Tpx family members were found in these cyanobacteria. The 129 Prx5 subfamily members were distributed across 127 cyanobacteria, and 65.5% of the sequenced cyanobacteria encoded at least one Prx5 (Fig. 5B and Fig. S5 and Table S5).

DISCUSSION

Here, we report the participation of PrxI in sulfane sulfur metabolism in cyanobacteria (Fig. 6). S₈ significantly induced the expression of all six *prxs* in PCC7002 (Fig. 1). Among them, we demonstrated that PrxI reduced S₈ to H₂S (Fig. 2) via the formation of an intramolecular disulfide bond between its Cys⁵³ and Cys¹⁵³ residues (Fig. 3). When *prxI* was partially inactivated, the PCC7002 mutant became more sensitive to S₈ (Fig. 4). These results support the idea that PCC7002 uses PrxI to deal with RSS stress.

Three experiments were designed to prove the function of Prxs in PCC7002: one using the purified Prxs-MBP (Fig. 2A), one using the cell lysate of *E. coli* expressing Prxs-MBP (Fig. 2B), and one using the resting cells of recombinant *E. coli* expressing Prxs-MBP (Fig. 2C). All three experiments indicated that only PrxI had the ability to reduce S₈. DTT was used as a reductant in the purified protein experiment. Even though DTT can directly react with S₈ to produce H₂S, the existence of PrxI in the reac-

FIG 5 Legend (Continued)

AhpC-Prx1 family, PrxIII PCC7002 and PrxV PCC7002 belonged to the BCP-PrxQ family, PrxIV PCC7002 belonged to the Prx6 family, and PrxVI PCC7002 belonged to the AphE family. The tree was an unrooted one. The candidates were analyzed by using ClustalW for alignment and MEGA 7.0 for neighbor-joining tree building with the following parameters: pairwise deletion, p-distance distribution, and bootstrap analysis of 1,000 repeats. (B) The fractions of cyanobacteria that carry the Prx5-type Prx. 127 of the 198 cyanobacteria genomes encoded Prx5-type Prx.

tion produced more H_2S (Fig. 2A). The maximum production of H_2S by purified PrxI was at 15 min, while that of the cell lysate was at 5 min. This may be due to the fact that DTT was a chemical reductant which could be much lower than the physiological reductant in the cell lysate (55). The maximum production of H_2S by the recombinant *E. coli* with PrxI-MBP was also at 15 min, which may be due to the slow transformation of S_8 to cells. Furthermore, the lysates of *E. coli* expressing PrxII-MBP and PrxIV-MBP, as well as the resting cells expressing PrxIV-MBP and PrxVI-MBP, had lower H_2S production. That may be due to the interaction of Prx with cellular components, as H_2S production was not decreased in the experiment with using purified proteins (Fig. 2A). Prxs may have the ability to metabolize H_2S in the presence of cellular components. It has been reported that Cu/Zn superoxide dismutase (SOD) catalyzed H_2S oxidation to form polysulfide (56). We deduced that Prx may also have that ability, and this needs to be explored in a further study.

Prxs are antioxidant enzymes that play an important role in redox homeostasis and in redox regulation (28, 29). The mechanism of H_2O_2 metabolism by Prxs has been well-studied (38, 43). The “peroxidative” cysteine of the catalytic site (C_p) attacks H_2O_2 and is oxidized to sulfenic acid (C_p -SOH) in the first step of the catalytic cycle. Then, the resolving cysteine (C_r) attacks the (C_p -SOH) to release an H_2O molecule and form a disulfide bond (C_p - C_r). Prxs are divided into three classes based on the way the sulfenic acid (C_p -SOH) is recycled back to a thiol (C_p -SH): typical 2-Cys Prxs, atypical 2-Cys Prxs, and 1-Cys Prxs. In the typical 2-Cys Prxs, the C_p -SOH from one subunit is attacked by the C_r from the other subunit, resulting in the formation of an inter-subunit disulfide bond. In the atypical 2-Cys Prxs, both the C_p and the C_r are contained in the same subunit, and the condensation reaction results in the formation of an intramolecular disulfide bond. The 1-Cys Prxs contain only C_p and are without C_r . The C_p and C_r residues of PCC7002 PrxI are Cys⁵³ and Cys¹⁵³, and they formed an intramolecular disulfide bond. A probable mechanism of sulfane sulfur reduction by PCC7002 PrxI is also proposed (Fig. 6) based on that of H_2O_2 metabolism, in which Cys⁵³ reacts with sulfane sulfur, such as S_8 , to produce a persulfide (Cys⁵³-SSH), and Cys¹⁵³ attacks Cys⁵³-SSH to form an intramolecular disulfide bond (Cys⁵³-Cys¹⁵³) and release H_2S . In summary, we deduced that PCC7002 PrxI belongs to the atypical 2-Cys Prx family based on its mechanism (37, 40, 43), while it belongs to the Prx5 subfamily based on the analysis by the Deacon Active Site Profiler tool (Fig. 5A).

All six Prxs in PCC7002 were induced by S_8 (Fig. 1). However, in this study, only PrxI had the S_8 reduction activity. According to a phylogenetic analysis (Fig. 5), PrxI belongs to a separate branch from the other Prxs in PCC7002, the Tpx subfamily, while the sequences near the C_p of the Tpx family are highly conserved (Fig. 5B), suggesting that this region may be the key site for sulfane sulfur reduction, which is also vital for H_2O_2 reduction. It remains to be investigated whether other Prxs, especially the Prx5-type Prxs, reduce sulfane sulfur. Our analysis showed that 65% of cyanobacteria encode Prx5-type Prx (Fig. 5B). These results indicate the widespread and important roles of Prx5-type Prx in cyanobacteria.

Prxs are most likely the primary enzymes responsible for maintaining intracellular sulfane sulfur homeostasis in cyanobacteria in anoxic or hypoxic conditions (21, 57). In aerobic conditions, PDO oxidizes sulfane sulfur to sulfite (24). Because the RSS stress is more severe in hypoxic conditions (5, 12), Prxs may play important roles in sulfane sulfur metabolism in anoxic or hypoxic conditions. The action of Prxs against RSS may have been preserved through evolution, as Prxs existed long before oxygen became abundant on Earth (48).

Prxs are known to participate in ROS metabolism (58). Here, we report that they are also involved in RSS metabolism. Cyanobacteria are the oldest surviving microorganisms, and they have experienced the transformation from an anaerobic environment on Earth to an aerobic environment (59, 60). Given the long history of cyanobacterial sulfur exposure, Prxs were most likely first used to resist RSS (5, 60). Interestingly, many of the strategies used against ROS stress, such as catalase, superoxide dismutase, and

OxyR, have also been shown to be involved in coping with RSS stress (20, 36, 56). Here, the expression levels of *prxs* in PCC7002 were not as sensitive to H₂O₂ induction as they were to induction by S₈ (Fig. 1C), which might be due to the activity of other H₂O₂ mitigating enzymes, such as catalase and superoxide dismutase. Furthermore, sulfane sulfur might also disturb H₂O₂ homeostasis by downregulating catalase, thereby affecting the expression pattern of *prx* (Fig. 1). In summary, there is a close relationship between the strategies for coping with ROS and RSS (15, 61).

The maintenance of sulfane sulfur homeostasis in cyanobacteria is of great importance. In aerobic conditions, sulfane sulfur is an important intracellular signaling molecule that is involved in the regulation of critical photosynthesis genes in cyanobacteria. Sulfane sulfur reduction by Prx would help maintain the normal physiology and photosynthesis of cyanobacteria (24). In hypoxia and darkness, elemental sulfur can be used as an electron receptor for sulfur-dependent respiration, which enables cyanobacteria to yield ATP via the fermentation of endogenous stored glycogen (3, 33). However, high concentrations of sulfane sulfur in this environment can also be toxic to cells, so Prx-mediated sulfane sulfur reduction is a key pathway for detoxification, as photosynthesis ceases and oxidation by PDO is excluded in hypoxia and darkness.

In summary, here, a Prx is shown for the first time to act as a sulfur reductase that reduces S₈ to H₂S. Also, cyanobacteria may use Prxs to deal with RSS stress. S₈ induced the expression of *prxs* in PCC7002, and PrxI worked effectively to reduce S₈ to H₂S, thereby improving the tolerance of PCC7002 to S₈. The conserved sequence of PrxI near residue C_p appears to be important for the activity of PrxI. Sulfane sulfur metabolism by Prxs could be the main strategy by which ancient cyanobacteria coped with RSS stress, which facilitated the survival of cyanobacteria in complex environments, especially oxygen-limited areas in the modern oceans.

MATERIALS AND METHODS

Strains and culture conditions. PCC7002 and its mutants were grown in conical flasks containing medium A (62), supplemented with 1 mg of NaNO₃ mL⁻¹ (designed as medium A⁺) under continuous illumination by 50 μmol photons m⁻² s⁻¹ at 30°C. Kanamycin (50 μg/mL) was used to select the *prxI* mutant. To explore the effect of O₂ concentrations, we cultured PCC7002 by bubbling with a mixture of O₂ and N₂, with O₂ contents of 2%, 10%, and 20%. *Escherichia coli* (*E. coli*) was cultured in Luria-Bertani (LB) medium at 37°C. The strains and plasmids used in this paper are listed in Table S1.

Induction, RNA extraction, and qRT-PCR analysis. PCC7002 cells in logarithmic growth with an OD_{730 nm} value of 0.6 to 0.7 were induced by S₈, H₂O₂, and O₂ under continuous illumination by 50 μmol photons m⁻² s⁻¹ at 30°C for 3 h. The cells were then harvested by centrifugation at 10,000 × *g* at 4°C for 10 min. Total RNA was isolated using the TaKaRa MiniBEST Universal RNA Extraction Kit, and the concentration of RNA was verified using a Qubit 4 instrument (Thermo Fisher). cDNA was produced using the Prime Script RT Reagent Kit with gDNA Eraser (TaKaRa, Beijing, China). The SYBR Premix *Ex Taq* II Kit (TaKaRa) was used for a quantitative reverse transcriptase polymerase chain reaction (qRT-PCR), and the reactions were run in a Light Cycler 480 II sequence detection system (Roche, Shanghai, China). Primers for target genes are given in Table S2. *mpA* (SYNPCC7002_A0989), encoding the protein subunit of RNase P (RNase P), was used as the reference gene (63). The results were analyzed according to the 2^{-ΔΔCT} method (64).

Overexpression of Prxs and enzyme activity determination. Recombinant Prxs were fused to the C-terminus of maltose binding protein (MBP) and were overexpressed using the vector pMal-C2X (65, 66). Whole fragments encoding *prxI-VI* were amplified from PCC7002 genomic DNA using primers pMal-*prxI-VI*-F/R. Then, the fragments were ligated with pMal-C2X and transformed into *E. coli* DH5α. The resulting plasmids were transformed into *E. coli* BL21 (DE3) to overexpress the recombinant Prx fusion proteins. *E. coli* BL21 (pMal-C2X) and *E. coli* BL21 (pMal-*prxs*) were cultured in LB at 37°C to an OD_{600 nm} of 0.6. Next, 0.5 mM isopropyl β-D-1-thiogalactopyranoside (IPTG) was added, and the cells were further cultivated at 30°C for 6 h. For resting cell analysis, cells were collected and resuspended in phosphate-buffered saline (PBS; 50 mM, pH 7.4) at an OD_{600 nm} of 10. Then, S₈ (200 μM) was added to initiate the reaction, and the release of H₂S was determined by the methylene blue method (67). Here, the S₈ was made by dissolving sulfur powder in acetone, in which it was soluble in the range of concentrations we used. For the analysis of cell lysates, the collected cells in PBS were disrupted using a pressure cell homogenizer (SPCH-18; Stansted Fluid Power Ltd., United Kingdom). The total protein content in the cell lysates was adjusted to 20 mg mL⁻¹, and SDS-PAGE was used to verify whether the lysates contained similar amounts of recombinant Prx. Again, 200 μM S₈ was added to start the reaction, and the release of H₂S was determined by the methylene blue method. For the analysis of the purified protein, induced cells were harvested and resuspended in binding buffer (20 mM Tris-HCl, 200 mM NaCl, 1 mM EDTA). Then, the cells were disrupted using a pressure cell homogenizer, and the mixture was centrifuged at 20,000 × *g* for 20 min to acquire crude cell extract. The crude extract was loaded onto amylose resin, and the target protein was eluted using the binding buffer containing 10 mM maltose. The eluted

protein solution was then loaded onto a PD-10 desalting column (GE) for buffer exchange to desalting buffer (20 mM NaH_2PO_4 , 10% glycerol, pH 7.6). The purified proteins were then resolved by SDS-PAGE. The reaction mixtures contained 100 $\mu\text{g}/\text{mL}$ Prx, 100 μM DTT, 200 μM S_8 , and 50 mM HEPES-NaOH (pH 7.0). The control containing DTT and S_8 but no Prx was included. The cysteine to serine mutants of Prx were generated using the primer pairs *prxl*-C53S-F/R, *prxl*-C78S-F/R, and *prxl*-C153S-F/R with a modified QuikChange site-directed mutagenesis method (68, 69). The reduction of S_8 by cell lysates of *E. coli* BL21 (pMal-*prxl* C53S), *E. coli* BL21 (pMal-*prxl* C78S), and *E. coli* BL21 (pMal-*prxl* C153S) was detected as described above.

Non-reducing SDS-PAGE. PrxI, PrxI C53S, PrxI C78S, and PrxI C153S with the MBP tag were purified in the same way as described above. PrxI, PrxI C53S, PrxI C78S, and PrxI C153S were released from the fusion with MBP by using Factor Xa at room temperature for 24 h. The released proteins were treated with 250 μM S_8 at 25°C for 30 min. After the S_8 treatment, 1 mM DTT was added to convert the modified thiols back to reduced thiols. No treatment and treatment with only 1 mM DTT were used as controls. The samples were then resolved by nonreducing SDS-PAGE, in which the loading buffer contained no DTT or other reducing agents.

Construction of the CstR reporter system. A CstR-based reporter plasmid was constructed by following a reported protocol to assess the ability of PrxI to metabolize sulfane sulfur (53). In *Staphylococcus aureus*, CstR (Copper-sensing operon repressor [CsoR]-like sulfurtransferase repressor) is a transcriptional repressor that represses the expression of the *cst* operon, which encodes a putative sulfide oxidation system, by binding to the OP1 and OP2 sites of the *cst* promoter (70). Here, CstR and the *cst* promoter with OP1 and OP2 sites were used to regulate the expression of *mkate* (encoding a red fluorescent protein, mKate). CstR represses the expression of *mkate*, but sulfane sulfur can act on CstR and depress the repression. In this way, the fluorescence intensity of mKate could be used to characterize the concentration of intracellular sulfane sulfur. We constructed plasmids with the *prxl* gene expressed, coupled behind the mKate-encoding gene. The *prxl* gene was cloned using primers *cstR*-*mkate*-*prxl*-F/R that contained 20-bp extensions overlapping the vector fragment. Then, the segments were connected with the CstR-OP1-mKate vector by using a TEDA assembly. The three cysteines in PrxI were all individually mutated to serine, using primer pairs *prxl*-C53S-F/R, *prxl*-C78S-F/R, and *prxl*-C153S-F/R, by a QuikChange site-directed mutagenesis to assess their roles. Correct CstR reporter plasmids were transformed into *E. coli* BL21 for experiments.

Construction of PCC7002 mutants. A *prxl* mutant of PCC7002 (PCC7002 Δ *prxl*-p) was constructed by homologous recombination as previously reported (24). Briefly, the primer sets *prx*-del-1/*prx*-del-2 and *prx*-del-5/*prx*-del-6 (Table S2) were used to acquire the upstream and downstream segments of the *prxl* gene by PCR from the genomic DNA of PCC7002. The lengths of the segments were about 1,000 bp.

The kanamycin resistance cartridge was amplified from pET30a using primers *prx*-del-3/*prx*-del-4. Long fragments coupling the upstream segment, the kanamycin resistance cartridge, and the downstream segment were obtained by fusion PCR. The fused fragment was connected with the pJET1.2 blunt vector by using the TEDA method (71), and then the resulting vector was transformed into *E. coli* DH5 α by electroporation. Correct transformants were verified by PCR and by sequencing. The correct plasmid was then transformed into PCC7002 by natural transformation. The final transformants were selected using kanamycin (50 $\mu\text{g}/\text{mL}$) and confirmed by PCR.

Toxicity analysis of sulfane sulfur. PCC7002 and PCC7002 Δ *prxl*-p in the logarithmic growth phase with an $\text{OD}_{730\text{ nm}}$ of 0.6 to 0.7 were treated with S_8 for 6 h in sealed centrifugation tubes. After incubation, the cells were washed and resuspended in fresh A^+ medium. The cells were diluted with A^+ medium to an $\text{OD}_{730\text{ nm}}$ of 0.05, and 10 μL were spread on an A^+ -agar plate. Differences between strains PCC7002 and PCC7002 Δ *prxl*-p were observed after cultivation at 30°C under continuous illumination by 50 photons $\text{m}^{-2}\text{ s}^{-1}$ for about 7 days. Furthermore, the growth curves of PCC7002 and PCC7002 Δ *prxl*-p were also monitored. S_8 was added to the medium at the beginning of the culturing.

Phylogenetic analysis. 198 cyanobacterial genomes were downloaded from the NCBI database (updated 17 December 2021). The query sequences of the Prxs were based on reported data (Table S3) (46). The Prx candidates in PCC7002 were analyzed by using ClustalW software for sequence alignment and MEGA 7.0 to build neighbor-joining phylogenetic trees. The parameters were: pairwise deletion, p distance distribution, and bootstrap analysis with 1,000 repeats.

Data availability. We will provide any strain and materials used in this study upon request.

SUPPLEMENTAL MATERIAL

Supplemental material is available online only.

FIG S1, TIF file, 1.9 MB.

FIG S2, TIF file, 2.8 MB.

FIG S3, TIF file, 2.6 MB.

FIG S4, TIF file, 2.2 MB.

FIG S5, TIF file, 2.3 MB.

TABLE S1, DOCX file, 0.02 MB.

TABLE S2, DOCX file, 0.02 MB.

TABLE S3, DOCX file, 0.02 MB.

TABLE S4, DOCX file, 0.02 MB.

TABLE S5, XLSX file, 0.03 MB.

ACKNOWLEDGMENTS

This work was financially supported by grants from the National Natural Science Foundation of China (grant no. 91951202) and the China Postdoctoral Science Foundation (grant no. 2021M691913). We thank Douglas A. Campbell from Mount Allison University and Judith M. Klatt from the Max Planck Institute for Marine Microbiology for constructive discussions.

We declare no conflict of interest.

REFERENCES

- de Beer D, Weber M, Chennu A, Hamilton T, Lott C, Macalady J, Klatt JM. 2017. Oxygenic and anoxygenic photosynthesis in a microbial mat from an anoxic and sulfidic spring. *Environ Microbiol* 19:1251–1265. <https://doi.org/10.1111/1462-2920.13654>.
- Huang S, Wilhelm SW, Harvey HR, Taylor K, Jiao N, Chen F. 2012. Novel lineages of *Prochlorococcus* and *Synechococcus* in the global oceans. *ISME J* 6:285–297. <https://doi.org/10.1038/ismej.2011.106>.
- Stal LJ, Moezelaar R. 1997. Fermentation in cyanobacteria. *FEMS Microbiology Rev* 21:179–211. [https://doi.org/10.1016/S0168-6445\(97\)00056-9](https://doi.org/10.1016/S0168-6445(97)00056-9).
- Merz E, Dick GJ, de Beer D, Grim S, Hübener T, Littmann S, Olsen K, Stuart D, Lavik G, Marchant HK, Klatt JM. 2021. Nitrate respiration and diel migration patterns of diatoms are linked in sediments underneath a microbial mat. *Environ Microbiol* 23:1422–1435. <https://doi.org/10.1111/1462-2920.15345>.
- Schunck H, Lavik G, Desai DK, Großkopf T, Kalvelage T, Löscher CR, Paulmier A, Contreras S, Siegel H, Holtappels M, Rosenstiel P, Schilhabel MB, Graco M, Schmitz RA, Kuypers MMM, Laroche J. 2013. Giant hydrogen sulfide plume in the oxygen minimum zone off Peru supports chemolithoautotrophy. *PLoS One* 8:e68661. <https://doi.org/10.1371/journal.pone.0068661>.
- Callbeck CM, Lavik G, Ferdelman TG, Fuchs B, Gruber-Vodicka HR, Hach PF, Littmann S, Schoffelen NJ, Kalvelage T, Thomsen S, Schunck H, Löscher CR, Schmitz RA, Kuypers MMM. 2018. Oxygen minimum zone cryptic sulfur cycling sustained by offshore transport of key sulfur oxidizing bacteria. *Nat Commun* 9:1729. <https://doi.org/10.1038/s41467-018-04041-x>.
- Kimura H. 2015. Signaling molecules: hydrogen sulfide and polysulfide. *Antioxid Redox Signal* 22:362–376. <https://doi.org/10.1089/ars.2014.5869>.
- Beauchamp RO, Jr., Bus JS, Popp JA, Boreiko CJ, Andjelkovich DA. 1984. A critical review of the literature on hydrogen sulfide toxicity. *Crit Rev Toxicol* 13:25–97. <https://doi.org/10.3109/10408448409029321>.
- Fukuto JM, Ignarro LJ, Nagy P, Wink DA, Kevil CG, Feelisch M, Cortese-Krott MM, Bianco CL, Kumagai Y, Hobbs AJ, Lin J, Ida T, Akaïke T. 2018. Biological hydropersulfides and related polysulfides - a new concept and perspective in redox biology. *FEBS Lett* 592:2140–2152. <https://doi.org/10.1002/1873-3468.13090>.
- Barton LL, Fardeau ML, Fauque GD. 2014. Hydrogen sulfide: a toxic gas produced by dissimilatory sulfate and sulfur reduction and consumed by microbial oxidation. *Met Nos Life Sci* 14:237–277. https://doi.org/10.1007/978-94-017-9269-1_10.
- Breitburg D, Levin LA, Oschlies A, Gregoire M, Chavez FP, Conley DJ, Garcon V, Gilbert D, Gutierrez D, Isensee K, Jacinto GS, Limburg KE, Montes I, Naqvi SWA, Pitcher GC, Rabalais NN, Roman MR, Rose KA, Seibel BA, Telszewski M, Yasuhara M, Zhang J. 2018. Declining oxygen in the global ocean and coastal waters. *Science* 359:eaam7240. <https://doi.org/10.1126/science.aam7240>.
- Canfield DE, Stewart FJ, Thamdrup B, De Brabandere L, Dalsgaard T, Delong EF, Revsbech NP, Ulloa O. 2010. A cryptic sulfur cycle in oxygen-minimum-zone waters off the Chilean coast. *Science* 330:1375–1378. <https://doi.org/10.1126/science.1196889>.
- Greiner R, Palinkas Z, Basell K, Becher D, Antelmann H, Nagy P, Dick TP. 2013. Polysulfides link H₂S to protein thiol oxidation. *Antioxid Redox Signal* 19:1749–1765. <https://doi.org/10.1089/ars.2012.5041>.
- Iciek M, Kowalczyk-Pachel D, Biłska-Wilkosz A, Kwiecień I, Górny M, Włodek L. 2016. S-sulphydration as a cellular redox regulation. *Bioscience Rep* 36:e00304. <https://doi.org/10.1042/BSR20150147>.
- Olson KR. 2020. Reactive oxygen species or reactive sulfur species: why we should consider the latter. *J Experimental Biology* 223:jeb196352. <https://doi.org/10.1242/jeb.196352>.
- Walsh BJC, Wang J, Edmonds KA, Palmer LD, Zhang Y, Trinidad JC, Skaar EP, Giedroc DP. 2020. The response of *Acinetobacter baumannii* to hydrogen sulfide reveals two independent persulfide-sensing systems and a connection to biofilm regulation. *mBio* 11:e01254-20. <https://doi.org/10.1128/mBio.01254-20>.
- Wang T, Ran M, Li X, Liu Y, Xin Y, Liu H, Liu H, Xia Y, Xun L. 2021. The pathway of sulfide oxidation to octasulfur globules in the cytoplasm of aerobic bacteria. *Applied Environ Microbiol* 88:e0194121.
- Xu Z, Qiu Z, Liu Q, Huang Y, Li D, Shen X, Fan K, Xi J, Gu Y, Tang Y, Jiang J, Xu J, He J, Gao X, Liu Y, Koo H, Yan X, Gao L. 2018. Converting organosulfur compounds to inorganic polysulfides against resistant bacterial infections. *Nature Communication* 9:3713. <https://doi.org/10.1038/s41467-018-06164-7>.
- Rai M, Ingle AP, Paralikar P. 2016. Sulfur and sulfur nanoparticles as potential antimicrobials: from traditional medicine to nanomedicine. *Expert Rev Anti Infect Ther* 14:969–978. <https://doi.org/10.1080/14787210.2016.1221340>.
- Hou N, Yan Z, Fan K, Li H, Zhao R, Xia Y, Xun L, Liu H. 2019. OxyR senses sulfane sulfur and activates the genes for its removal in *Escherichia coli*. *Redox Biol* 26:101293. <https://doi.org/10.1016/j.redox.2019.101293>.
- Hamilton TL, Klatt JM, de Beer D, Macalady JL. 2018. Cyanobacterial photosynthesis under sulfidic conditions: insights from the isolate *Leptolyngbya* sp. strain hensonii. *ISME J* 12:568–584. <https://doi.org/10.1038/ismej.2017.193>.
- Klatt JM, Haas S, Yilmaz P, de Beer D, Polerecky L. 2015. Hydrogen sulfide can inhibit and enhance oxygenic photosynthesis in a cyanobacterium from sulfidic springs. *Environ Microbiol* 17:3301–3313. <https://doi.org/10.1111/1462-2920.12791>.
- Klatt JM, Al-Najjar MA, Yilmaz P, Lavik G, de Beer D, Polerecky L. 2015. Anoxygenic photosynthesis controls oxygenic photosynthesis in a cyanobacterium from a sulfidic spring. *Appl Environ Microbiol* 81:2025–2031. <https://doi.org/10.1128/AEM.03579-14>.
- Liu D, Zhang J, Lü C, Xia Y, Liu H, Jiao N, Xun L, Liu J. 2020. *Synechococcus* sp. strain PCC7002 uses sulfide:quinone oxidoreductase to detoxify exogenous sulfide and to convert endogenous sulfide to cellular sulfane sulfur. *mBio* 11:e03420-19. <https://doi.org/10.1128/mBio.03420-19>.
- Ran M, Wang T, Shao M, Chen Z, Liu H, Xia Y, Xun L. 2019. Sensitive method for reliable quantification of sulfane sulfur in biological samples. *Anal Chem* 91:11981–11986. <https://doi.org/10.1021/acs.analchem.9b02875>.
- Liu H, Xin Y, Xun L. 2014. Distribution, diversity, and activities of sulfur dioxygenases in heterotrophic bacteria. *Appl Environ Microbiol* 80:1799–1806. <https://doi.org/10.1128/AEM.03281-13>.
- Xin Y, Liu H, Cui F, Liu H, Xun L. 2016. Recombinant *Escherichia coli* with sulfide:quinone oxidoreductase and persulfide dioxygenase rapidly oxidizes sulfide to sulfite and thiosulfate via a new pathway. *Environ Microbiol* 18:5123–5136. <https://doi.org/10.1111/1462-2920.13511>.
- Oktyabrsky ON, Smirnova GV. 2007. Redox regulation of cellular functions. *Biochemistry (Mosc)* 72:132–145. <https://doi.org/10.1134/s0006297907020022>.
- Holmgren A. 1989. Thioredoxin and glutaredoxin systems. *J Biol Chem* 264:13963–13966. [https://doi.org/10.1016/S0021-9258\(18\)71625-6](https://doi.org/10.1016/S0021-9258(18)71625-6).
- Sato I, Shimatani K, Fujita K, Abe T, Shimizu M, Fujii T, Hoshino T, Takaya N. 2011. Glutathione reductase/glutathione is responsible for cytotoxic elemental sulfur tolerance via polysulfide shuttle in fungi. *J Biol Chem* 286:20283–20291. <https://doi.org/10.1074/jbc.M111.225979>.
- Dóka É, Pader I, Biró A, Johansson K, Cheng Q, Ballagó K, Prigge JR, Pastor-Flores D, Dick TP, Schmidt EE, Arnér ES, Nagy P. 2016. A novel persulfide detection method reveals protein persulfide- and polysulfide-reducing functions of thioredoxin and glutathione systems. *Sci Adv* 2:e1500968. <https://doi.org/10.1126/sciadv.1500968>.
- Schwedt A, Kreutzmann A-C, Polerecky L, Schulz-Vogt HN. 2011. Sulfur respiration in a marine chemolithoautotrophic beggiatoa strain. *Front Microbiol* 2:276–276. <https://doi.org/10.3389/fmicb.2011.00276>.

33. Moezelaar R, Bijvank SM, Stal LJ. 1996. Fermentation and sulfur reduction in the mat-building cyanobacterium *Microcoleus chthonoplastes*. *Appl Environ Microbiol* 62:1752–1758. <https://doi.org/10.1128/aem.62.5.1752-1758.1996>.
34. Mueller S, Riedel HD, Stremmel W. 1997. Direct evidence for catalase as the predominant H₂O₂-removing enzyme in human erythrocytes. *Blood* 90:4973–4978. <https://doi.org/10.1182/blood.V90.12.4973>.
35. Nandi A, Yan LJ, Jana CK, Das N. 2019. Role of catalase in oxidative stress- and age-associated degenerative diseases. *Oxid Med Cell Longev* 2019: 9613090. <https://doi.org/10.1155/2019/9613090>.
36. Olson KR, Gao Y, DeLeon ER, Arif M, Arif F, Arora N, Straub KD. 2017. Catalase as a sulfide-sulfur oxidoreductase: an ancient (and modern?) regulator of reactive sulfur species (RSS). *Redox Biol* 12:325–339. <https://doi.org/10.1016/j.redox.2017.02.021>.
37. Dietz KJ. 2011. Peroxiredoxins in plants and cyanobacteria. *Antioxid Redox Signal* 15:1129–1159. <https://doi.org/10.1089/ars.2010.3657>.
38. Rhee SG, Chae HZ, Kim K. 2005. Peroxiredoxins: a historical overview and speculative preview of novel mechanisms and emerging concepts in cell signaling. *Free Radic Biol Med* 38:1543–1552. <https://doi.org/10.1016/j.freeradbiomed.2005.02.026>.
39. Rocha S, Gomes D, Lima M, Bronze-da-Rocha E, Santos-Silva A. 2015. Peroxiredoxin 2, glutathione peroxidase, and catalase in the cytosol and membrane of erythrocytes under H₂O₂-induced oxidative stress. *Free Radic Res* 49:990–1003. <https://doi.org/10.3109/10715762.2015.1028402>.
40. Zhang L, Lu Z. 2015. Expression, purification and characterization of an atypical 2-Cys peroxiredoxin from the silkworm, *Bombyx mori*. *Insect Mol Biol* 24:203–212. <https://doi.org/10.1111/imb.12149>.
41. Pérez-Pérez ME, Mata-Cabana A, Sánchez-Riego AM, Lindahl M, Florencio FJ. 2009. A comprehensive analysis of the peroxiredoxin reduction system in the Cyanobacterium *Synechocystis* sp. strain PCC 6803 reveals that all five peroxiredoxins are thioredoxin dependent. *J Bacteriol* 191:7477–7489. <https://doi.org/10.1128/JB.00831-09>.
42. Sun CC, Dong WR, Zhao J, Nie L, Xiang LX, Zhu G, Shao JZ. 2015. Cysteine-independent catalase-like activity of vertebrate Peroxiredoxin 1 (Prx1). *J Biol Chem* 290:19942–19954. <https://doi.org/10.1074/jbc.M115.659011>.
43. Wood ZA, Schroder E, Robin Harris J, Poole LB. 2003. Structure, mechanism and regulation of peroxiredoxins. *Trends in Biochemistry Science* 28:32–40. [https://doi.org/10.1016/S0968-0004\(02\)00003-8](https://doi.org/10.1016/S0968-0004(02)00003-8).
44. Si M, Wang T, Pan J, Lin J, Chen C, Wei Y, Lu Z, Wei G, Shen X. 2017. Graded response of the multifunctional 2-cysteine peroxiredoxin, CgPrx, to increasing levels of hydrogen peroxide in *Corynebacterium glutamicum*. *Antioxid Redox Signal* 26:1–14. <https://doi.org/10.1089/ars.2016.6650>.
45. Monteiro G, Horta BB, Pimenta DC, Augusto O, Netto LES. 2007. Reduction of 1-Cys peroxiredoxins by ascorbate changes the thiol-specific antioxidant paradigm, revealing another function of vitamin C. *Proc Natl Acad Sci U S A* 104:4886–4891. <https://doi.org/10.1073/pnas.0700481104>.
46. Nelson KJ, Knutson ST, Soito L, Klomsiri C, Poole LB, Fetrow JS. 2011. Analysis of the peroxiredoxin family: using active-site structure and sequence information for global classification and residue analysis. *Proteins* 79: 947–964. <https://doi.org/10.1002/prot.22936>.
47. Poole LB, Nelson KJ. 2016. Distribution and features of the six classes of peroxiredoxins. *Mol Cells* 39:53–59. <https://doi.org/10.14348/molcells.2016.2330>.
48. Knoop B, Loumaye E, Van Der Eecken V. 2007. Evolution of the peroxiredoxins. *Subcell Biochem* 44:27–40. https://doi.org/10.1007/978-1-4020-6051-9_2.
49. Stramma L, Prince ED, Schmidtko S, Luo J, Hoolihan JP, Visbeck M, Wallace DWR, Brandt P, Körtzinger A. 2012. Expansion of oxygen minimum zones may reduce available habitat for tropical pelagic fishes. *Nat Clim Chang* 2:33–37. <https://doi.org/10.1038/nclimate1304>.
50. Hallam SJ, Torres-Beltran M, Hawley AK. 2017. Monitoring microbial responses to ocean deoxygenation in a model oxygen minimum zone. *Sci Data* 4: 170158. <https://doi.org/10.1038/sdata.2017.158>.
51. Diaz RJ, Rosenberg R. 2008. Spreading dead zones and consequences for marine ecosystems. *Science* 321:926–929. <https://doi.org/10.1126/science.1156401>.
52. Ludwig M, Bryant DA. 2012. *Synechococcus* sp. strain PCC 7002 transcriptome: acclimation to temperature, salinity, oxidative stress, and mixotrophic growth conditions. *Front Microbiol* 3:354. <https://doi.org/10.3389/fmicb.2012.00354>.
53. Liu H, Fan K, Li H, Wang Q, Yang Y, Li K, Xia Y, Xun L. 2019. Synthetic gene circuits enable *Escherichia coli* to use endogenous H₂S as a signaling molecule for quorum sensing. *ACS Synth Biol* 8:2113–2120. <https://doi.org/10.1021/acssynbio.9b00210>.
54. Watanabe S, Ohbayashi R, Shiwa Y, Noda A, Kanesaki Y, Chibazakura T, Yoshikawa H. 2012. Light-dependent and asynchronous replication of cyanobacterial multi-copy chromosomes. *Mol Microbiol* 83:856–865. <https://doi.org/10.1111/j.1365-2958.2012.07971.x>.
55. Horta BB, de Oliveira MA, Discola KF, Cussiol JR, Netto LE. 2010. Structural and biochemical characterization of peroxiredoxin Qbeta from *Xylella fastidiosa*: catalytic mechanism and high reactivity. *J Biol Chem* 285: 16051–16065. <https://doi.org/10.1074/jbc.M109.094839>.
56. Olson KR, Gao Y, Arif F, Arora K, Patel S, DeLeon ER, Sutton TR, Feelisch M, Cortese-Krott MM, Straub KD. 2018. Metabolism of hydrogen sulfide (H₂S) and production of reactive sulfur species (RSS) by superoxide dismutase. *Redox Biol* 15:74–85. <https://doi.org/10.1016/j.redox.2017.11.009>.
57. Vaquer-Sunyer R, Duarte CM. 2008. Thresholds of hypoxia for marine biodiversity. *Proc Natl Acad Sci U S A* 105:15452–15457. <https://doi.org/10.1073/pnas.0803833105>.
58. Storz G, Jacobson FS, Tartaglia LA, Morgan RW, Silveira LA, Ames BN. 1989. An alkyl hydroperoxide reductase induced by oxidative stress in *Salmonella typhimurium* and *Escherichia coli*: genetic characterization and cloning of ahp. *J Bacteriol* 171:2049–2055. <https://doi.org/10.1128/jb.171.4.2049-2055.1989>.
59. Dorr M, Kassbohrer J, Grunert R, Kreisler G, Brand WA, Werner RA, Geilmann H, Apfel C, Robl C, Weigand W. 2003. A possible prebiotic formation of ammonia from dinitrogen on iron sulfide surfaces. *Angew Chem Int Ed Engl* 42: 1540–1543. <https://doi.org/10.1002/anie.200250371>.
60. Soo RM, Hemp J, Parks DH, Fischer WW, Hugenholtz P. 2017. On the origins of oxygenic photosynthesis and aerobic respiration in Cyanobacteria. *Science* 355:1436–1440. <https://doi.org/10.1126/science.aal3794>.
61. Olson KR. 2019. Hydrogen sulfide, reactive sulfur species and coping with reactive oxygen species. *Free Radic Biol Med* 140:74–83. <https://doi.org/10.1016/j.freeradbiomed.2019.01.020>.
62. Stevens SE, Porter RD. 1980. Transformation in *Agmenellum quadruplicatum*. *Proc Natl Acad Sci U S A* 77:6052–6056. <https://doi.org/10.1073/pnas.77.10.6052>.
63. Szekeres E, Sicora C, Dragoş N, Drugă B. 2014. Selection of proper reference genes for the cyanobacterium *Synechococcus* PCC 7002 using real-time quantitative PCR. *FEMS Microbiol Lett* 359:102–109. <https://doi.org/10.1111/1574-6968.12574>.
64. Livak KJ, Schmittgen TD. 2001. Analysis of relative gene expression data using real-time quantitative PCR and the 2- $\Delta\Delta$ CT method. *Methods* 25:402–408. <https://doi.org/10.1006/meth.2001.1262>.
65. Waugh DS. 2016. The remarkable solubility-enhancing power of *Escherichia coli* maltose-binding protein. *Postepy Biochem* 62:377–382. https://doi.org/10.18388/pb.2016_41.
66. Zhao X, Li G, Liang S. 2013. Several affinity tags commonly used in chromatographic purification. *J Anal Methods Chem* 2013:581093. <https://doi.org/10.1155/2013/581093>.
67. Hughes MN, Centelles MN, Moore KP. 2009. Making and working with hydrogen sulfide: the chemistry and generation of hydrogen sulfide in vitro and its measurement in vivo: a review. *Free Radic Biol Med* 47: 1346–1453. <https://doi.org/10.1016/j.freeradbiomed.2009.09.018>.
68. Xia Y, Chu W, Qi Q, Xun L. 2015. New insights into the QuikChange process guide the use of Phusion DNA Polymerase for site-directed mutagenesis. *Nucleic Acids Res* 43:e12. <https://doi.org/10.1093/nar/gku1189>.
69. Xia Y, Xun L. 2017. Revised mechanism and improved efficiency of the Quikchange site-directed mutagenesis method. *Methods Mol Biol* 1498: 367–374. https://doi.org/10.1007/978-1-4939-6472-7_25.
70. Luebke JL, Shen J, Bruce KE, Kehl-Fie TE, Peng H, Skaar EP, Giedroc DP. 2014. The CsoR-like sulfurtransferase repressor (CstR) is a persulfide sensor in *Staphylococcus aureus*. *Mol Microbiol* 94:1343–1360. <https://doi.org/10.1111/mmi.12835>.
71. Xia Y, Li K, Li J, Wang T, Gu L, Xun L. 2019. T5 exonuclease-dependent assembly offers a low-cost method for efficient cloning and site-directed mutagenesis. *Nucleic Acids Res* 47:e15–e15. <https://doi.org/10.1093/nar/gky1169>.